Geophysical Research Letters

Supporting Information for【Extratropical intraseasonal signals along the subtropical westerly jet as a window of opportunity for subseasonal prediction over East Asia in boreal summer】

Tao Zhu[1,2]　Jing Yang[1,2]

[1] Key Laboratory of Environmental Change and Natural Disaster, Beijing Normal University, Beijing 100875, China

[2] Faculty of Geographical Science, Beijing Normal University, Beijing 100875, China

Submitted to GRL

Nov. 2022

**Corresponding author address: Jing Yang, Key Laboratory of Environmental Change and Natural Disaster, Faculty of Geographical Science, Beijing Normal University, 19#Xinjiekouwai Street, Haidian District, Beijing 100875, China. E-mail: yangjing@bnu.edu.cn*

1. Four Tables, six Figures, and two equations

Table S1. Description of the S2S models.

	Time range	**Resolution**	**Re-forecast**	**Rfc length**	**Rfc frequency**	**Rfc size**
CMA	Days 0–60	~1° × 1°, L40	Fixed	1994–2014	Daily	4
ECCC	Days 0–32	0.45° × 0.45°, L40	On the fly	1995–2014	Weekly	4
ECMWF	Days 0–46	T639/319 L91	On the fly	1996–2015	2/week	11
ISAC-CNR	Days 0–31	0.8° × 0.56°, L54	Fixed	1981–2010	Every 5 days	5
Meteo-France	Day 0–60	~0.5° × 0.8°, L85	On the fly	1993–2014	4/month	15
NCEP	Days 0–44	~1° × 1°, L64	Fixed	1999–2010	Daily	4

Table S2. ROC contingency table for defining event probabilistic prediction parameters.

Bin number	**Prediction probabilities**	**Observed occurrences**	**Observed non-occurrences**
1	$0–P_2$ (%)	O_1	NO_1
2	$P_2–P_3$ (%)	O_2	NO_2
3	$P_3–P_4$ (%)	O_3	NO_3
……	……	……	……
n	$P_n–P_{n+1}$ (%)	O_n	NO_n
……	……	……	……
N	$P_N–100$ (%)	O_N	NO_N

In ROC contingency table, *n* is the number of the n^{th} probability interval or bin *n*. *n* goes from *1* to *N*. *Pn* is the lower probability limit for bin *n*; P_{n+1} is upper probability limit for bin *n*; *N* is the number of probability intervals or bins. The prediction probabilities are the member sizes in each model that predict the event occurrence in this study.

$$O_n = \sum w_i(O)_i;\ NO_n = \sum w_i(NO)_i$$

where O_n/NO_n is the observed occurred/non-occurred frequency in n^{th} probability interval, i is the samples, and w_i is $\cos\theta_i$, representing the weight coefficient of the i^{th}, in which θ_i is the latitude of i^{th}. O_i is 1 when an event corresponding to a prediction in n^{th} probability interval, is observed as an occurrence, otherwise O_i is 0. NO_i is 1 when an event corresponding to a predicion in n^{th} probability interval, is not observed, otherwise NO_i is 0.

The curve formed by the hit rate (HR) and false alarm rate (FAR) is the ROC curve, in which the HR and FAR are calculated as

$$HR_n = \sum_{i=n}^{N} O_i / \sum_{i=1}^{N} O_i;\ FAR_n = \sum_{i=n}^{N} NO_i / \sum_{i=1}^{N} NO_i$$

Table S3. Sample sizes in EISO-SJ-S and EISO-SJ-W summers before and after removing the ENSO/MJO/BSISO-associated summers.

Name	EISO-SJ-S	EISO-SJ-W	Sample numbers for EISO-SJ-S and EISO-SJ-W	EISO-SJ-S⁻	EISO-SJ-W⁻	Sample numbers for EISO-SJ-S⁻ and EISO-SJ-W⁻
ERA-Interim	1986, 1988, 2004, 2005, 2007, 2009, 2011, 2013	1984, 1994, 1995, 1998, 2003, 2008, 2010, 2012, 2018	\	2005, 2009, 2013	1984, 1994, 1998, 2003, 2012, 2018	\
CMA	2004, 2005, 2007, 2009, 2011, 2013	1994, 1995, 1998, 2008, 2010, 2012	738 (6 year × 123 times year^{-1})	2005, 2009, 2013	1994, 1998, 2012	369 (3 year × 123 times year^{-1})
ECCC	2004, 2005, 2007, 2009, 2011, 2013	1995, 1998, 2003, 2008, 2010, 2012	102 (6 year × 17 times year^{-1})	2005, 2009, 2013	1998, 2003, 2012	51 (3 year × 17 times year^{-1})
ECMWF	2004, 2007, 2009, 2011, 2013	1998, 2003, 2008, 2010, 2012	175 (5 year × 35 times year^{-1})	2005, 2009, 2013	1998, 2003, 2012	105 (3 year × 35 times year^{-1})
ISAC-CNR	1986, 1988, 2004, 2005, 2007, 2009	1984, 1994, 1995, 1998, 2008, 2010	150 (6 year × 25 times year^{-1})	2005, 2009	1984, 1998	50 (2 year × 25 times year^{-1})
Meteo-France	2004, 2005, 2007, 2009, 2011, 2013	1994, 1995, 1998, 2008, 2010, 2012	96 (6 year × 16 times year^{-1})	2005, 2009, 2013	1994, 1998, 2012	48 (3 year × 16 times year^{-1})
NCEP	2004, 2007, 2009	2003, 2008, 2010	369 (3 year × 123 times year^{-1})	2009	2003	123 (1 year × 123 times year^{-1})

*EISO-SJ-S⁻ and EISO-SJ-W⁻ are the strong and weak EISO-SJ intensity summers, respectively, without the ENSO/MJO/BSISO-associated summers. ENSO-related summers are defined as the absolute values of the boreal summer averaged Oceanic Niño Index (ONI) index are larger than 0.5, MJO-related summers are that the absolute values of the normalized boreal summer averaged MJO amplitude, calculated by $\sqrt{RMM1^2 + RMM2^2}$, are large than 1, and BSISO-related summers are that the absolute value of the normalized boreal summer averaged BSISO amplitude (i.e., BSISO1 index), is large than 1. ONI index is obtained via https://origin.cpc.ncep.noaa.gov/products/analysis_monitoring/ensostuff/ONI_v5.php, RMM1 and RMM2 are via http://www.bom.gov.au/climate/mjo/, and BSISO1 index is via https://apcc21.org/ser/meth.do?lang=en.

Table S4. The fractional variance of quasi-biweekly and synoptic SAT and precipitation over the ETP, SWB and NC.

	SAT		**Precipitation**	
	quasi-biweekly	synoptic	quasi-biweekly	synoptic
ETP	36.0%	13.0%	35.2%	33.3%
SWB	45.3%	19.9%	33.3%	41.1%
NC	36.1%	23.2%	27.2%	43.1%

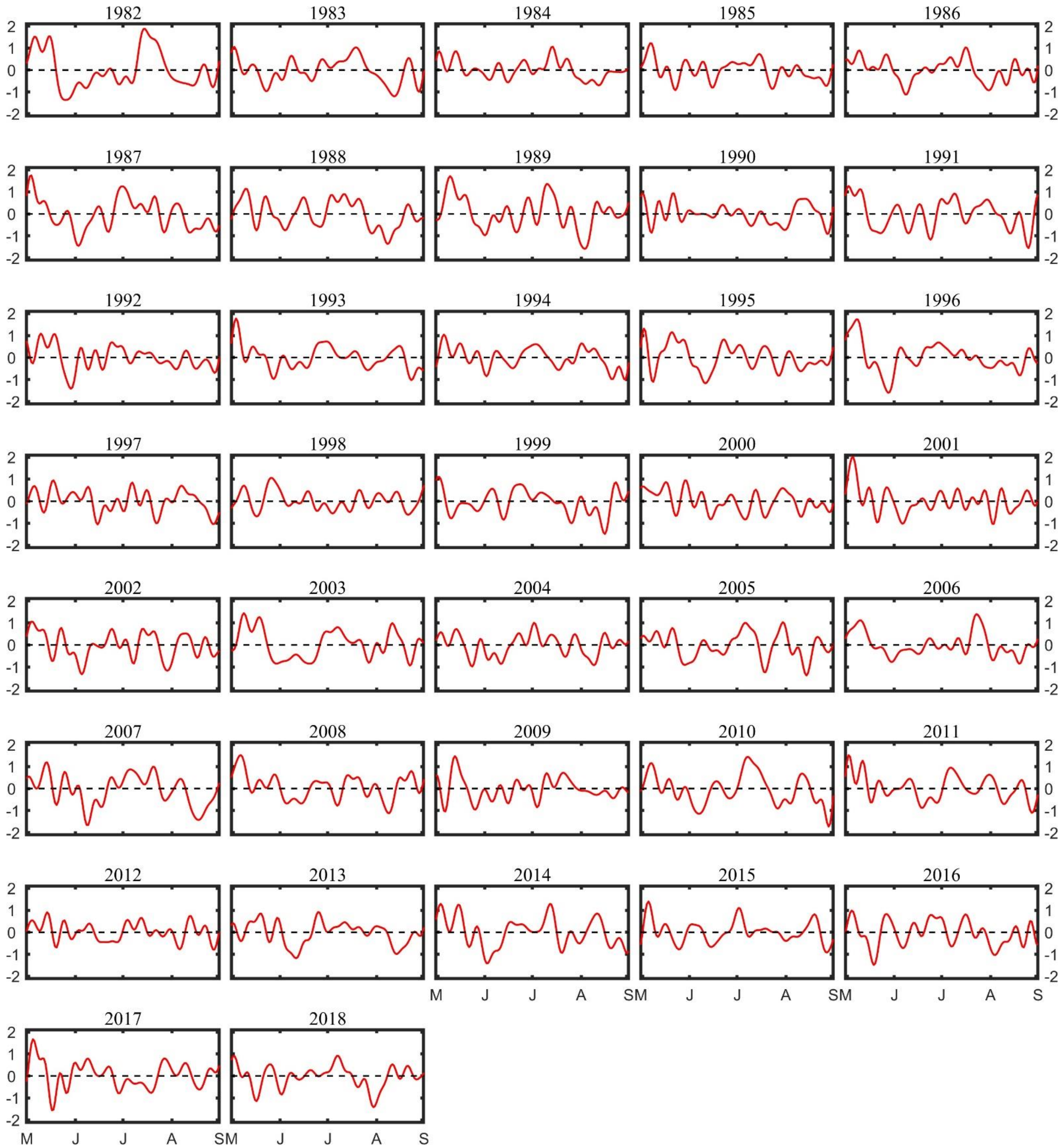

FIG. S1. Time series of the intraseasonal SJ index during each boreal summer (MJJA) of the 37 years.

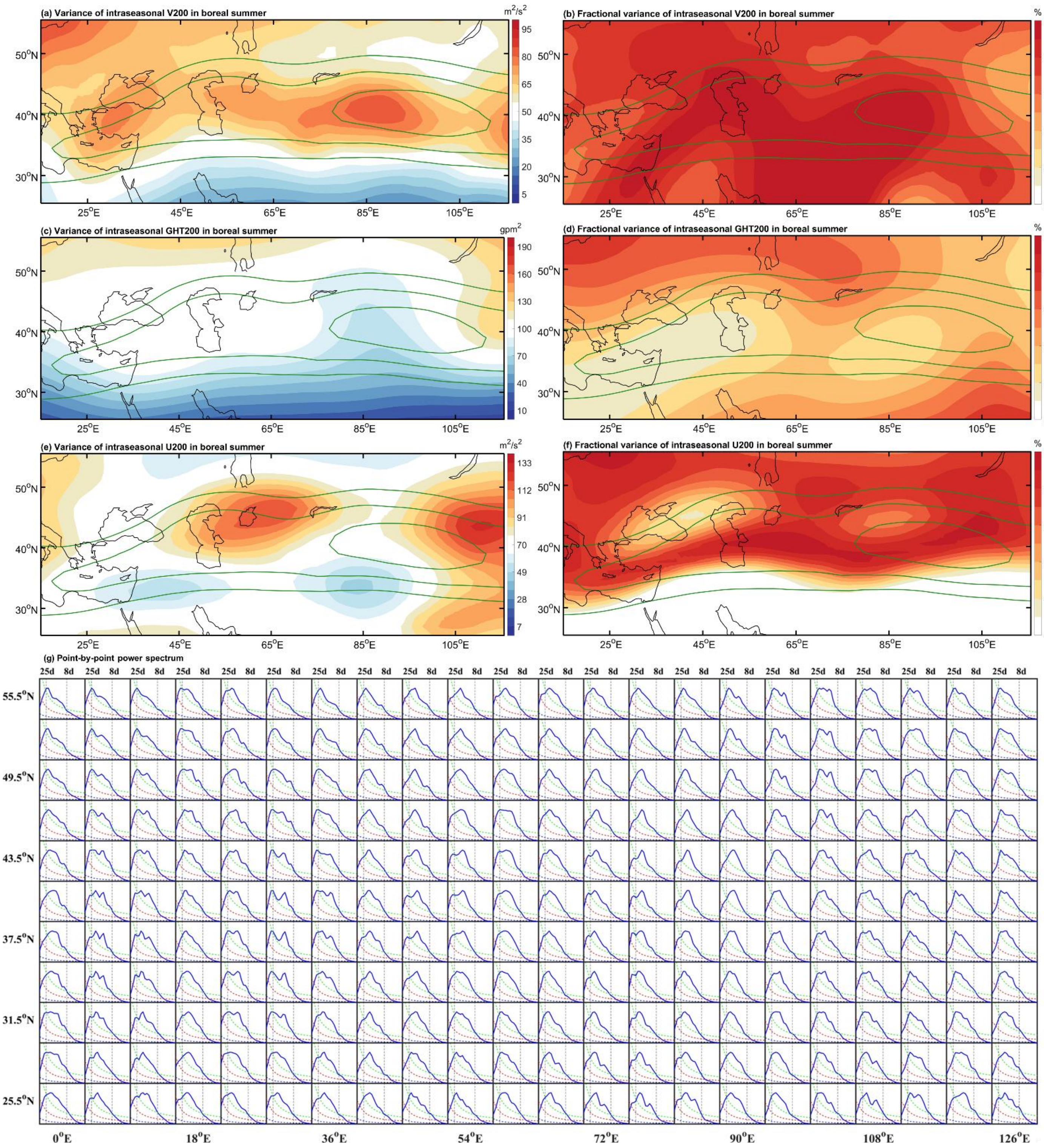

FIG. S2. (a) Variance (shading; unit: m^2 s^{-2}) and **(b)** fractional variance (shading; unit: %) of intraseasonal V200 against total V200 variance in boreal summer. Green lines are the summer–mean U200 contour of 18, 23 and 28 m s^{-1}, which broadly denote the SJ's location. **(c, d)**/**(e, f)** As in **(a, b),** but for GHT200/U200. **(g)** The point-by-point power spectrum of intraseasonal V200 over the SJ region. The red dashed line denotes the Markov red noise spectrum, and the blue/green dashed line represents the a priori/a posteriori 99% confidence. The grid point is chosen at intervals of 4.5 degrees of longitude and 3 degrees of latitude.

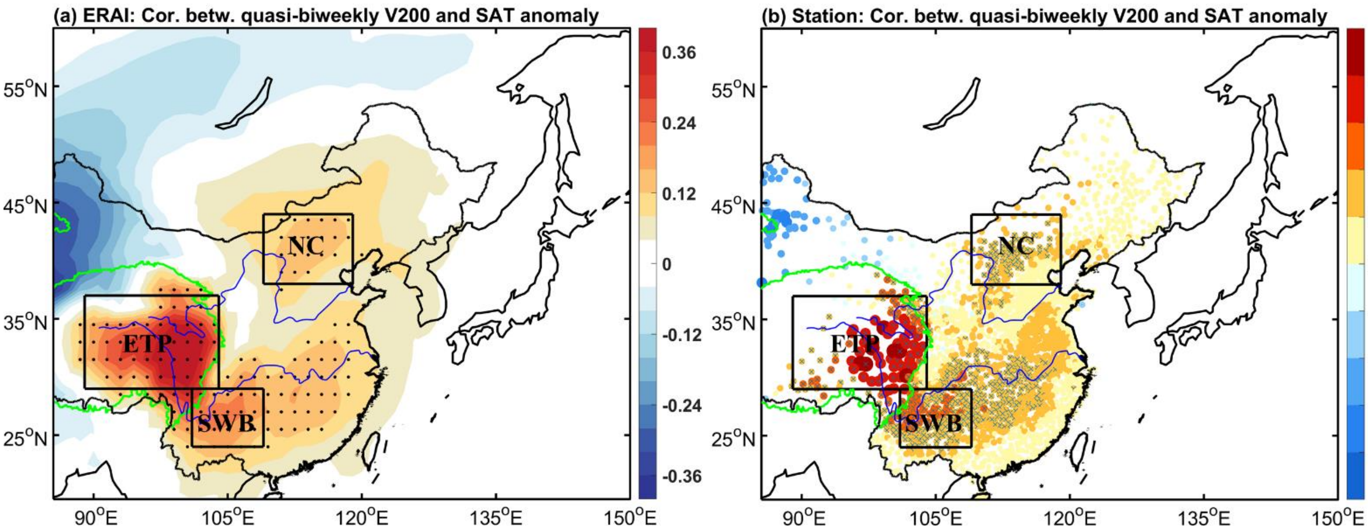

FIG. S3. Correlation coefficients (shading) between the quasi-biweekly V200 and anomalous SAT obtained from the **(a)** ERA Interim (ERAI) and **(b)** 2479-gauge stations. Black dots in **(a)** and blue "x" in **(b)** show the results above the 90% confidence level.

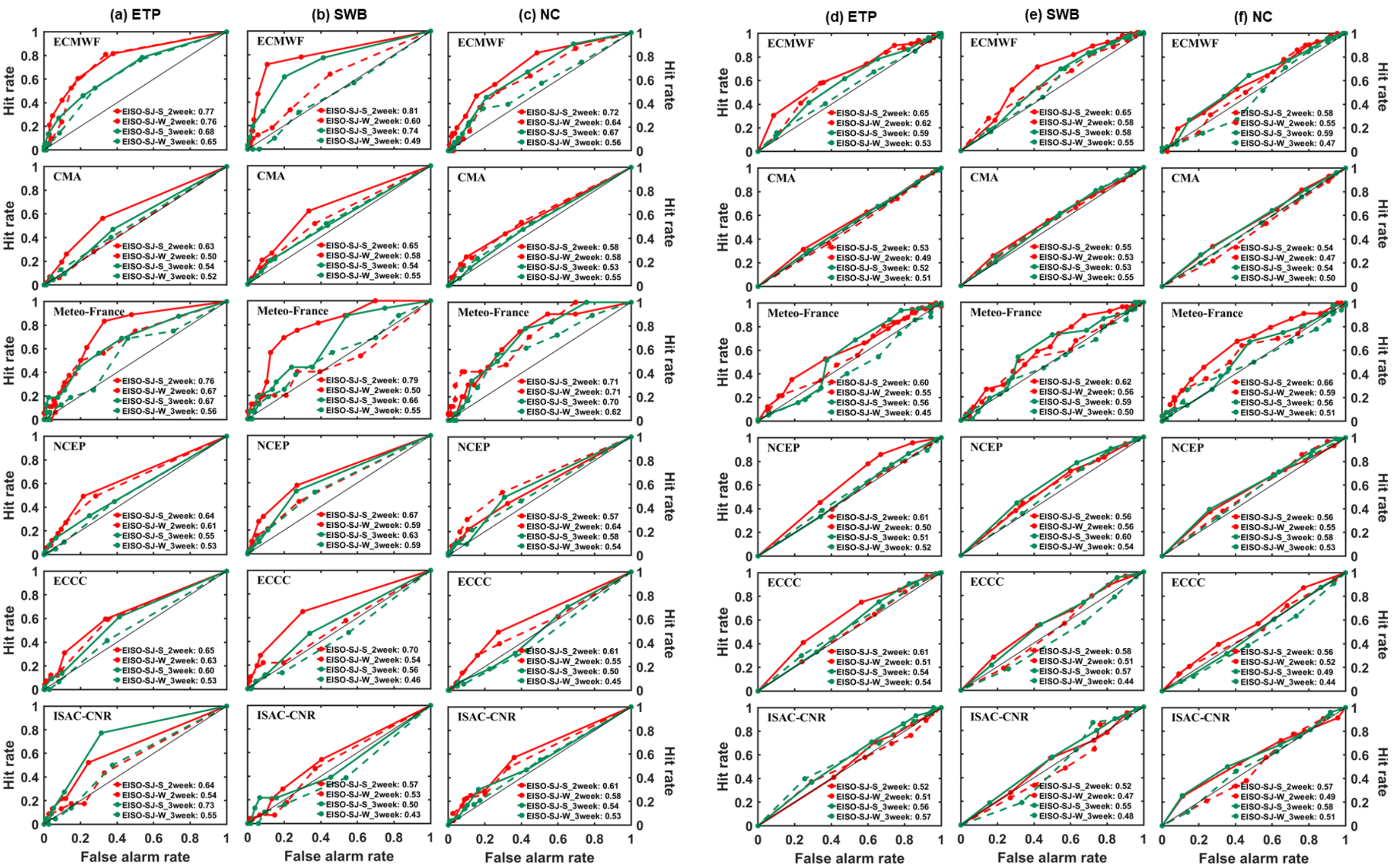

FIG. S4. Relative operating characteristics (ROC) curve for predicting below-normal SAT events over the **(a)** ETP, **(b)** SWB and **(c)** NC from S2S models with two- and three-week lead times. **(d–f)** As in **(a–c)**, but for normal SAT events. Here the below-normal SAT events are defined as the weekly SAT anomaly of <–1 °C, and the normal SAT event is the weekly SAT anomaly between –1 °C and 1 °C.

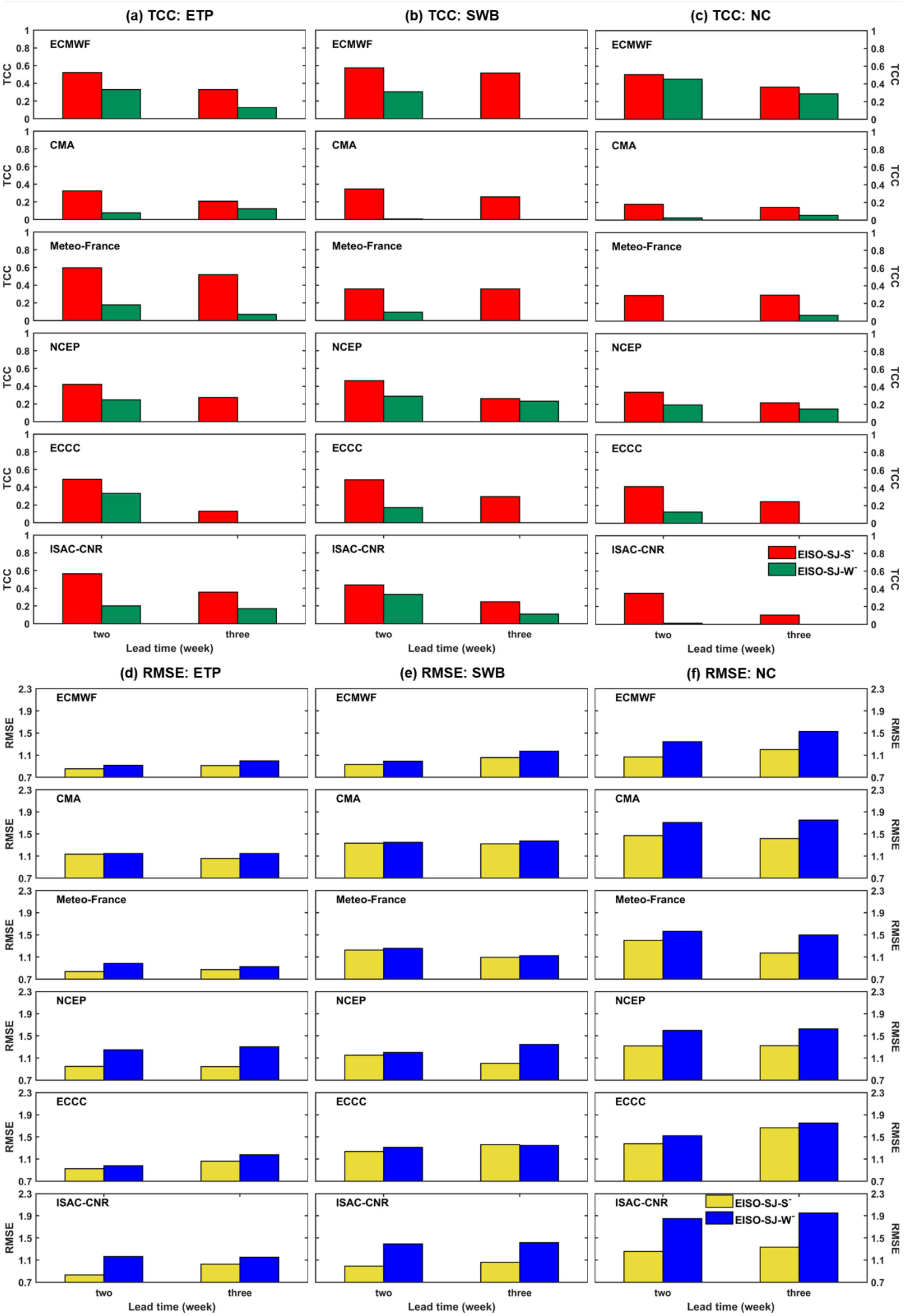

FIG. S5. Temporal correlation coefficient (TCC) between the observed weekly SAT anomaly and predicted ensemble-mean weekly SAT anomaly over the **(a)** ETP, **(b)** SWB and **(c)** NC with two- and three-week lead times. EISO-SJ-S^{-} and EISO-SJ-W^{-} samples are the prediction results in strong and weak EISO-SJ intensity summers, respectively, without the ENSO/MJO/BSISO-associated summers. **(d–f)** As in **(a–c)**, but for Root Mean Square Error (RMSE).

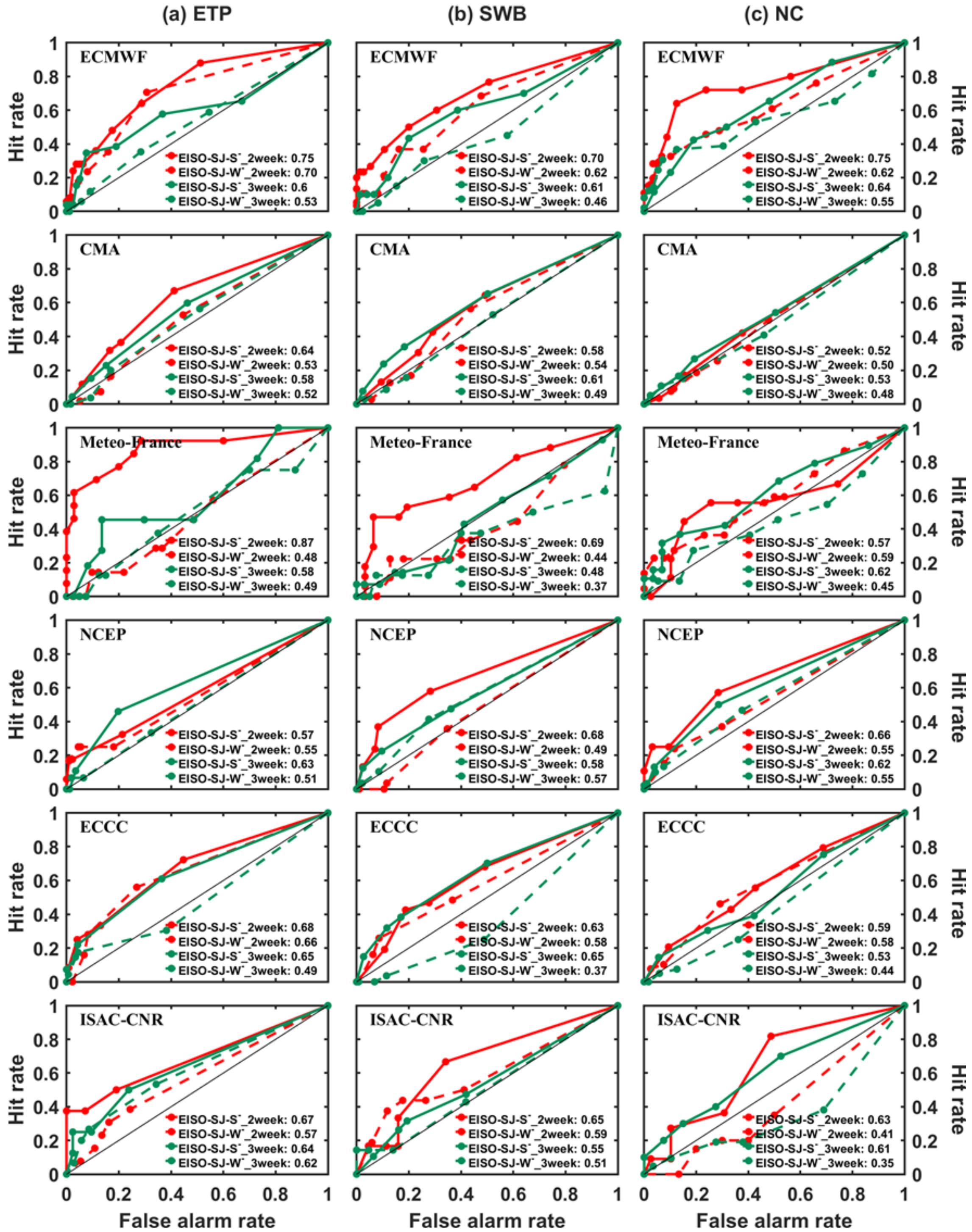

FIG. S6. ROC curve for predicting above-normal SAT events over the **(a)** ETP, **(b)** SWB and **(c)** NC from S2S models with two- and three-week lead times. EISO-SJ-S⁻ and EISO-SJ-W⁻ samples are the prediction results in strong and weak EISO-SJ intensity summers, respectively, without the ENSO/MJO/BSISO-associated summers.

$$TCC = \frac{\sum_{i=1}^{N}(x_i \times f_i)}{\sqrt{\sum_{i=1}^{N} x_i{}^2}\sqrt{\sum_{i=1}^{N} f_i{}^2}} \tag{S1}$$

$$\mathrm{RMSE} = \sqrt{\frac{1}{N}\sum_{i=1}^{N}(x_i - f_i)^2} \tag{S2}$$

where N, x_i and f_i are the sample numbers, observed and predicted ensemble-mean weekly anomaly (SAT & precipitation), respectively.